The Single Fiber Composite Test: A Comparison of E-Glass Fiber Fragmentation Data with Statistical Theories

Gale A. Holmes, Jae Hyun Kim, Stefan Leigh, Walter McDonough

Polymers Division, National Institute of Standards and Technology, Gaithersburg, Maryland 20899-8541

Received 19 November 2007; accepted 25 October 2008
DOI 10.1002/app.31002
Published online 22 March 2010 in Wiley InterScience (www.interscience.wiley.com).

ABSTRACT: The exact theories advanced by Curtin[6] and Hui et al.[7] to describe the fiber break evolution process in single fiber composites are found to be incorrect when compared with experimental data. In contrast to theoretical predictions where the matrix is assumed to be elastic perfectly plastic, experimental data indicate that the sizes of the fragment lengths that survive to saturation decrease as the strain is increased. It is also shown that the break locations at saturation are uniform along the length of the fiber specimens, with the uniformity apparently being independent of interfacial shear strength, fiber type, matrix type, and fiber–fiber interactions. The theory of uniform spacings gives an explicit distribution function for the ordered fragment lengths. © 2010 Wiley Periodicals, Inc. J Appl Polym Sci 117: 509–516, 2010

Key words: glass fibers; polymer-matrix composites (PMCS); fragmentation; interface; statistics

INTRODUCTION

The interest in the single fiber fragmentation test (SFFT) methodology lies in the use of the test outputs to quantify the interfacial shear strength (IFSS), which is a fundamental property used to characterize the level of adhesion between the fiber and the matrix in composites. This property is thought to be obtainable from micromechanical tests such as the SFFT. Currently, the SFFT methodology provides only a relative means of quantifying the performance of formulations designed to promote adhesion between the fiber and matrix. The outputs from this test methodology have been used to quantify composite performance and model composite failure behavior. Due to the importance of this test, there is an extensive literature on this subject and the embedded fiber fragmentation test (EFFT) methodologies, including single fiber and multifiber array configurations, which have evolved in the last decade to become potential tools for quantifying the impact of fiber–fiber interaction and its impact on critical flaw nucleation in composites.[1]

In a recent publication, Kim et al.[2] analyzed experimental data from the sequential fragmentation of E-glass fibers embedded in single fiber composite (SFC) specimens using the SFFT methodology, with the primary result being that the fiber break locations evolve to a uniform distribution as saturation is approached. This result implies that the ordered spacings (i.e., fragment lengths) at saturation are modeled by a cumulative distribution function (CDF) described by (1).[3,4]

$$\Pr(D_{(n-j)} \le x) = \sum_{r=0}^{j} \binom{n}{r} \sum_{s=0}^{n-r} (-1)^s \binom{n-r}{s} [1-(r+s)x]_+^{n-1} \quad (1)$$

where $0 < x < 1$ and $a_+ = \max(a,0)$ (i.e., fiber length is 1), n denotes the total number of breaks over the U[0,1] length, $D_{(n-j)}$ denotes the $(n-j)^{th}$ fragment length.

These results contrast with the experimental results obtained by Gulino and Phoenix[5] from three-fiber hybrid microcomposites where a 5.5 μm graphite fiber was sandwiched between two 13-μm SK glass fibers with an interfiber distance of (3 ± 1) μm along the specimen length. From their data, the final fragment length distribution and the evolution of the fiber break density with increasing stress conformed to Weibull distributions. Curtin[6] noted that he expected the distribution of breaking stresses to conform to a Weibull at low stresses but did not understand the basis for agreement over such a wide range of stress. The results of Kim et al. indicate that the wide agreement observed in the Gulino and Phoenix data may in fact not be universal. This result is important since only the Gulino and Phoenix experimental data provide support for the theories[6,7] that have been advanced to quantify the

Correspondence to: G. A. Holmes (gale.holmes@nist.gov).

physics of the sequential fragmentation process that occurs in the SFFT.

It is important to note that the theories and the supporting Monte Carlo simulations assume that the matrix is elastic-perfectly plastic (EPP). Although this assumption has been repeatedly shown to be incorrect[8,9] for most polymer matrices, the EPP assumption is generally considered to be a reasonable approximation for capturing the key features of the sequential fragmentation process in the SFFT methodology. The EPP assumption leads to the conclusion that the smallest breaks in the final fragment length distribution are formed early in the test when the critical transfer length is shortest. This assumption anchors the filtered distribution concept that was advanced by Curtin[6] to develop his theory and found to be plausible by Hui et al.[7] in the development of their theory. The experimental data published by Kim et al. on E-glass SFCs showed the opposite effect, so that the filtered distribution concept utilized by the two theories cannot be applied to the Kim et al. data.

In addition to casting doubt upon the universality of the theories, the Kim et al. data suggest that the physics of the sequential fragmentation process may not be well-enough understood to reliably predict composite failure behavior since the key input parameters are obtained from the EFFT methodologies. As an example, these composite failure models indicate that the density of fiber breaks increases as the interfiber distance between fibers decreases. Results by Li et al.[10] on micromechanics specimens composed of 2D Nicalon multifiber arrays, and later confirmed by Kim and Holmes[11] on 2D E-glass multifiber arrays, indicate that the break density along the length of a fiber decreases as the interfiber distance decreases. This result contradicts the prediction arrived at from shear lag models derived by Cox[12] and others.[13,14]

Therefore, the Kim et al. and Li et al. experimental results indicate that additional investigations are required of the EFFT methodologies to determine the efficacy of these approaches in assessing interfacial phenomena in composite materials, in providing useful input parameters for composite failure models, and in assessing critical flaw nucleation in composite materials. In this article, the fragmentation of embedded E-glass fibers is further investigated by assessing the impact of the matrix type, IFSS, and fiber–fiber interactions on the evolution of the sequential fiber fragmentation process.

For completeness, the relative break locations that occurred in SFCs tested by the 2nd VAMAS (the Versailles Project on Advanced Materials and Standards) Round Robin testing protocol[15] are fitted to the uniform distribution function to illuminate differences that may arise between the sequential fragmentation of E-glass/DGEBA/*m*-PDA specimens and carbon fiber/DGEBA/*m*-PDA specimens, where DGEBA denotes the diglycidyl ether of bisphenol-A and *m*-PDA denotes *meta*-phenylenediamine.

EXPERIMENTAL

Unsized E-glass fibers, $\sim$ 15 μm in diameter, were obtained from Owens Corning.* The fibers were either used as received (bare E-glass fibers) or treated with the *n*-octadecyl triethoxysilane (NOTS)[16] or glycidyloxypropyl trimethoxysilane (GOPS), with the GOPS surface treatment performed by the procedure given in Ref. 17. The AS-4 carbon fibers were obtained from the Hexcel Corporation.[15]

The mold preparation procedure and curing procedure for the E-Glass SFCs made using the diglycidyl ether of bisphenol-A (DGEBA) resin (Epon 828, Shell) cured with *meta*-phenylenediamine (*m*-PDA, Fluka, or Sigma-Aldrich) have been published previously by Holmes et al.[9,15,16,18,19] McDonough et al.[20] have described the procedure for preparing the polyisocyanurate SFCs, and Kim et al.[21] have described the procedure for preparing the combinatorial microcomposite SFC specimens used in this report. The AS-4 carbon fiber SFC specimens were prepared by Rich et al. using the procedure described in Ref. 15.

The testing protocols for the E-glass SFC specimens are most completely described in Ref. 18 and the test protocol associated with the AS-4 SFC specimens is described in Ref. 15. Finally, the automated testing procedure used for the combinatorial microcomposites has been previously described by Kim et al.[11,21] The standard uncertainty in determining the break locations was determined to be 1.1 μm, whereas the standard uncertainty in the reported fragment lengths is 1.6 μm.[16]

RESULTS AND DISCUSSIONS

The effects of matrix behavior, adhesion strength, and testing rate on uniform break formation in E-glass SFCs

The locations of the fiber breaks along the length of an E-glass fiber embedded in a SFC composed of DGEBA/*m*-PDA epoxy resin conform to a uniform distribution, where the probability plot correlation coefficients of the break locations for the uniform distribution from multiple samples were consistently greater than or equal to 0.999 (Fig. 1). From the

*Certain commercial materials and equipment are identified in this paper to specify adequately the experimental procedure. In no case does such identification imply recommendation or endorsement by the National Institute of Standards and Technology, nor does it imply necessarily that the product is the best available for the purpose.

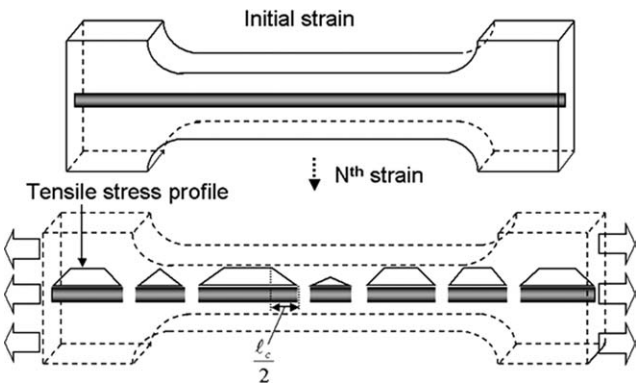

Figure 1 Schematic representation of fiber fragments occurring in the single fiber fragmentation test.

statistical theory of spacings, this result leads to the conclusion that the ordered distribution of the spacings (i.e., fragment lengths) produced by a SFFT conforms to (1).

To assess the generality of the Kim et al. results, single bare (i.e., unsized) E-glass fibers were embedded in a polyisocyanurate matrix and tested using fast, intermediate, and slow test protocols.[18] In contrast to the bare E-glass DGEBA/*m*-PDA SFC specimens, the fiber break densities of these specimens were unaffected by the testing rate. However, analyses of the break locations from these specimens indicate that they conform, like the DGEBA/*m*-PDA SFC specimens, to a uniform distribution as saturation is approached with probability plot correlation coefficients greater than 0.999. Consistent with the behavior observed in the bare E-glass DGEBA/*m*-PDA SFC specimens, the break locations evolve to a uniform distribution at fiber break densities of $\sim$ 21 breaks/cm and remain uniform for the remainder of the test, with break densities on the order of 30 breaks/cm being observed (Fig. 2).

To span the range of interfacial shear strengths, tests were also performed on E-glass fibers treated with *n*-octadecyl triethoxysilane (NOTS) and glycidyloxypropyl triethoxysilane (GOPS) that were also embedded in the DGEBA/*m*-PDA matrix. As expected the NOTS SFC specimens exhibited a marked reduction in the fiber break density at saturation since the *n*-octadecyl group does not covalently bond to the DEGBA/*m*-PDA matrix. For the four specimens tested, the saturation break densities ranged from (13 to 17) breaks/cm, significantly lower than those observed for the bare E-glass fibers tested in the DGEBA/*m*-PDA and polyisocyanurate matrices. Despite these low-break densities, the fiber break locations at saturation conformed in each specimen to a uniform distribution with probability plot correlation coefficients ranging from 0.9972 to 0.9994 for the four specimens tested (Fig. 2). For the NOTS data depicted in Figure 2, a uniform distribution fit (ppcc $>$ 0.99) was initially achieved at less than 12 breaks/cm.

Analysis of the GOPS SFC specimens showed that uniform distributions of fiber break locations were also achieved at saturation, correlations from (0.9990 to 0.9997), with break densities at the end of the test varying from (19.4 to 26.3) breaks/cm (Fig. 2). The onset of uniformity in these specimens occurred between 16 and 26 breaks/cm. Therefore, 94.7% of the 19 E-glass samples analyzed yield break locations that are strongly modeled by a uniform distribution, with the set with one outlier coming from the NOTS treated E-glass SFC samples, yielding a correlation coefficient for the fiber breaks fitted to a uniform distribution of 0.9972. These results indicate that the expected outcome from the sequential fragmentation of E-glass fiber SFCs at saturation are break locations that correspond to a uniform distribution, with standard statistics spacing theories indicating that the ordered spacings (i.e., fragment lengths) at saturation conform to the distribution function given in (1).

These results appear to contradict the experimental data of Gulino and Phoenix who studied the sequential fragmentation of carbon fiber hybrid microcomposites. However, it is worthwhile noting that all of the E-glass SFCs tested by Holmes et al. exhibited debonded regions whose total length comprised less than 5% of the total sample length. As an example, the NOTS SFC specimens yielded the largest average debond regions around each fiber break ($\sim$ 26 μm), with the range of the values for the four specimens being between (11 and 37) μm. Therefore, the debond regions occurring in the fracture of

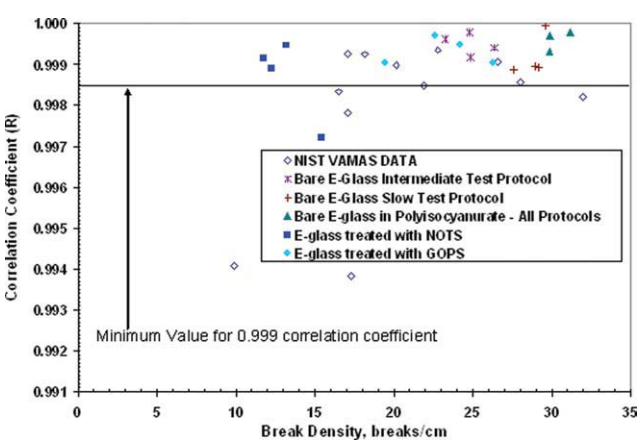

Figure 2 Correlation coefficients for probability plot fit of fiber break locations at saturation to the uniform distribution. (a) Solid symbols: E-Glass fiber SFCs with various surface treatments (bare, NOTS, and GOPS), test protocols (fast, intermediate, and slow), and matrices (DGEBA/*m*-PDA epoxy and polyisocyanurate). (b) Open symbols: AS-4 carbon fiber SFCs in DGEBA/*m*-PDA tested by fast (or VAMAS) testing protocol.[15] [Color figure can be viewed in the online issue, which is available at www.interscience.wiley.com.]

typical E-glass SFC specimens are significantly less than the (85 to 130) μm debond regions observed by Gulino and Phoenix, even though these researchers achieved break densities at saturation of 25 and 15 breaks/cm.

From a brief review of the literature on the silane treatment of glass fibers,[19] the minimal debonding in the NOTS SFC composites may be due to a predominant mechanical interlocking stress transfer mechanism at the fiber matrix interface caused by the interpenetration of the epoxy matrix into the porous silane surface treatment. Furthermore, the porous surface treatment that occurs when the glass fiber is treated with GOPS is also accompanied by the establishment of covalent bonds between the matrix and silane coupling agent, thereby providing a more efficient stress transfer mechanism than observed with the NOTS surface treatment. In Ref. 19, Holmes et al. showed that removal of the mechanical interlocking mechanism by treatment of the smooth glass surfaces with self-assembled monolayers of *n*-octadecyl trichlorosilane resulted in extensive debonding like that observed in carbon fiber composites, where the mechanical interlocking mechanism is based on the surface roughness of the carbon fiber. These results and observations suggest that in the absence of extensive debonding, the physics of the sequential fiber fragmentation process in E-glass fibers leads to a uniform distribution at saturation over a wide range of adhesion strengths, with the phenomenon appearing to be independent of matrix type.

Nonideal fragmentation behavior in E-glass fiber SFCs

Although it is known that most matrices used in the SFFT do not conform to the EPP assumption,[8,9] it is generally believed that the actual fragmentation process is consistent with this approximation. On the basis of assumed behavior, Curtin[6] formulated his theory of the fiber fragmentation process by viewing fiber fragmentation as occurring in two parts: (i) those fragments formed by breaks separated by more than $l\{\sigma\}$, the critical transfer length at the current stress level σ and (ii) those fragments smaller than $l\{\sigma\}$ formed at an earlier stress level $\sigma' < \sigma$ where a shorter $l\{\sigma'\} < l\{\sigma\}$ prevailed. Consequently, the filtered length distribution of fragment lengths in part (i) that contain all fragments larger than $l\{\sigma\}$ are viewed as being the same as that for a fiber with a unique strength, σ, whose effective fiber length is $L_T - L_R$, where L_T denotes the total length of the fiber and L_R represents the combined lengths of all fragments smaller than $l\{\sigma\}$. Hui et al.[7] in the development of their theory viewed the filtered length distribution approach used by Curtin as plausible, since their formulation also relies on the stress dependent and well-defined $l\{\sigma\}$ afforded by the EPP assumption. However, they took issue with the value of the maximum achievable packing density along the broken fiber, stating that the value should be one rather than the value of 0.7476 used by Curtin.

In a previous publication by Kim et al.,[2] it is shown for a bare E-glass fiber embedded in a DGEBA/*m*-PDA matrix that the smallest fragments in the final fragment length distribution were not formed at the beginning of the test, as theorized by Curtin and Hui et al., but rather at the end of the test. Consistent with these results, the size of the fragments surviving to saturation were found to decrease in size as the test progressed, in apparent contradiction to a $l\{\sigma\}$ based on the EPP assumption where the theories indicate that the size of the fragments surviving to saturation should increase as the strain in the SFC is increased. Furthermore, the Kelly-Tyson approximation of the critical transfer length ($l_c = 482$ μm for the Bare2_9 SFC specimen), also suggested that saturation was not achieved, since there were five fragments whose length ranged from 488 to 527 μm. This observation was somewhat surprising since fragments of length 462 and 482 μm fractured near the end of the test, with the shorter fragment being less than the Kelly-Tyson estimate of l_c. It should also be noted that the largest surviving fragments were formed early enough to undergo at least six additional increases in strain.

To better understand the fragmentation observed in the SFC by Kim et al., the SFFT fragment evolution data from the SFCs composed of a bare E-glass fiber embedded in a polyisocyanurate matrix (Table I) were analyzed. For the representative data shown in Table I, the Kelly-Tyson estimate of l_c is 420 μm which is ∼ 13% smaller than what was observed in the bare E-Glass/DGEBA/*m*-PDA SFC analyzed by Kim et al. Even with this reduction in the critical transfer length, four fragments were also found to exceed l_c, with the range being 445 to 508 μm. Note that the range of unbroken fragments that exceed l_c is comparable to the range of the five fragment lengths (488 to 527 μm) that exceeded l_c in the bare E-glass DGEBA/*m*-PDA SFC specimens even though the average fragment length at saturation in the bare E-glass polyisocyanurate SFC specimen is 13% shorter than observed in the bare E-glass DGEBA/*m*-PDA SFC specimen. Interestingly, saturation was indicated for the bare E-glass polyisocyanurate SFC specimen by the absence of fracture in three strain increments at the end of the test (4.41 to 4.80%). Consistent with the results obtained for the E-glass DGEBA/*m*-PDA SFC specimen, the size of the fragments surviving until saturation for the polyisocyanurate SFC specimen decreased with increasing strain.

TABLE I
Fragment Evolution Pattern from PU04E03 Test Specimen

Break density (breaks/cm)	0	1.9	2.5	3.7	8.7	12.5	15.0	19.9	21.2	23.1	23.7	24.3	25.5	26.8	28.7	30.5	31.2
% δ_c	2.0	7.8	9.8	13.7	29.4	41.2	49.0	64.7	68.6	74.5	76.5	78.4	82.4	86.3	92.2	98.0	100.0
Number of fragments	1	4	5	7	15	21	25	33	35	38	39	40	42	44	47	50	51
% Strain	1.42	1.49	1.62	1.73	1.79	1.95	2.05	2.26	2.37	2.55	2.99	3.16	3.28	3.62	3.78	4.17	4.41
Fragment no.	Fragment lengths given in μm																
10	16048	6064	4397	1631	1631	1631	1632	793	793	446	446	446	446	446	446	446	446
11										347	347	347	347	347	347	347	347
12								508	508	508	508	508	508	508	508	508	508
13								330	330	330	330	330	330	330	330	330	330
14				2766	956	372	372	372	372	372	372	372	372	372	372	372	372
15						584	584	584	584	584	584	584	584	584	245	245	245
16															339	339	339
17					1057	1057	1057	507	507	507	507	507	507	214	214	214	214
18														293	293	293	293
19								550	550	550	550	550	329	329	329	329	329
20													221	221	221	221	221
21					753	753	753	381	381	381	381	381	381	381	381	381	381
22								372	372	372	372	372	372	372	372	372	372
23			1667	1667	767	767	767	767	314	314	314	314	314	314	314	314	314
24									453	453	453	453	453	453	453	237	237
25																216	216
26					900	548	548	548	548	548	548	548	548	548	271	271	271
27															277	277	277
28						352	352	352	352	352	352	352	352	352	352	352	352
29		1597	1597	1597	351	351	351	351	351	351	351	351	351	351	351	351	351
30					1246	681	681	681	329	329	329	329	329	329	329	329	329
31									351	351	351	351	351	351	351	351	351
32						565	565	565	565	565	565	333	333	333	333	333	333
33												232	232	232	232	232	232
34		1881	1881	1881	458	458	458	458	458	458	458	458	458	458	458	458	458
35					692	692	692	692	692	313	313	313	313	313	313	313	313
36										379	379	379	379	379	379	379	379
37					731	283	283	283	283	283	283	283	283	283	283	283	283
38						448	448	448	448	448	448	448	448	448	448	209	209
39																239	239
40		6506	6506	2309	1406	1406	603	603	603	603	603	603	299	299	299	299	299
41													304	304	304	304	304
42							491	491	491	491	491	491	491	491	491	491	491
43							312	312	312	312	312	312	312	312	312	312	312
44					903	903	903	299	299	299	299	299	299	299	299	299	299
45								604	604	604	311	311	311	311	311	311	311
46											293	293	293	293	293	293	293
47				4197	680	281	281	281	281	281	281	281	281	281	281	281	281
48						399	399	399	399	399	399	399	399	399	399	399	399
49					3517	1185	647	341	341	341	341	341	341	341	341	341	341
50								307	307	307	307	307	307	307	307	307	307
51							538	538	538	538	538	538	538	538	538	538	275
52																	263
53						2331	1479	536	536	536	536	536	536	536	305	305	305
54															231	231	231
55								406	406	406	406	406	406	406	406	406	406
56								536	536	536	536	536	536	240	240	240	240
57														296	296	296	296
58							852	852	852	276	276	276	276	276	276	276	276
59										577	577	577	577	577	577	277	277
60																300	300

Plots of the average size of fragments surviving to saturation for the bare E-glass/DGEBA/*m*-PDA specimen (Bare2_9), the bare E-Glass/polyisocyanurate specimen (PU04E03), and the NOTS_D1 SFC specimens are shown in Figure 3. For the Bare2_9 and NOTS_D1 plots, one standard deviation error bars are shown at the strain increments where multiple fragments survived to saturation. For visual

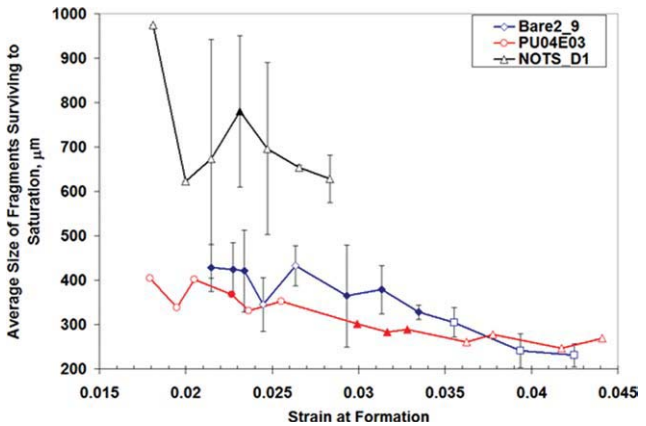

Figure 3 Plots of average sizes of fragments surviving to saturation from SFC specimens composed of E-glass fibers treated with *n*-octadecyl triethoxysilane (NOTS_D1) and bare E-glass fibers embedded in DGEBA/*m*-PDA (Bare2_9) and polyisocyanurate (PU04E03) matrices. The error bars represent one standard deviation for the multiple fragments formed at a give strain increment. To maintain clarity in the graph, the error bars for the PU04E03 specimen are not shown, but are comparable to those for the Bare2_9 specimen. Groupings for ANOVA analysis are formed by alternating between open and solid symbols. For a given data set, the point where a group becomes distinguishable from the previous group is represented by a change of symbol (e.g., circles change to triangles for the PU04E03 specimen). [Color figure can be viewed in the online issue, which is available at www.interscience.wiley.com.]

clarity, error bars were omitted for the PU04E03 specimen, but are comparable to those given for the Bare2_9 SFC specimen. It should be noted that the dispersion data for the polyisocyanurate specimen is extractable from the fragment evolution data provided in Table I.

Analysis of variance (ANOVA) analyses on each specimen depicted in Figure 3 were performed by dividing the fragments into three to five groups. The groupings are indicated in Figure 3 for each specimen by the alternation between open and solid symbols as the strain is increased. For the Bare2_9 specimen, the first three groups (upto $\sim$ 3.5% strain) were indistinguishable at the 95% confidence level with a P value of 0.15. The fourth grouping for the Bare2_9 data set, delineated by open squares, was distinguishable from the third grouping, delineated by solid diamonds, at the same confidence level with a P value of 0.008. In a similar manner, the first three groupings ($<$ 0.2.9% strain) of the polyisocyanurate SFC specimen (PU04E03) were indistinguishable with a P value of 0.72. However, the fourth grouping was distinguishable from the third at the 95% confidence level with a P value of 0.04, whereas the fourth and fifth groupings were indistinguishable with a P value of 0.10.

Although the data from these two specimens indicate a general downward trend in the size of the fragments surviving to saturation as the strain is increased, both sets of data suggest a rather sharp transition as indicated by the ANOVA analyses where the sizes of the fragments become decidedly smaller as the strain in the SFC specimen is increased. Interestingly, ANOVA analyses of the data from the NOTS_D1 SFC specimen shown in Figure 3 indicate that from the three groupings the average size of the fragments lengths surviving to saturation are indistinguishable at the 95% confidence level with a P value of 0.48. The sizes of the fragments surviving to saturation appear to remain constant as saturation is approached. These results suggest that adhesion strength and stress build-up in the fiber break regions may have a significant impact on the formation of small fragment lengths as saturation is approached.

The uniform distribution and fiber break locations from carbon fiber SFC specimens

In 2000, the 2nd round robin assessment of the SFFT was conducted under the auspices of VAMAS. Approximately 100 AS-4 carbon fiber/DGEBA/*m*-PDA SFC specimens were prepared in five batches by the Michigan State University Composites Laboratory.[15] The National Institute of Standards and Technology (NIST) randomized the samples from these batches and distributed them to seven laboratories for testing. In Figure 2, the correlation coefficients of the break locations from 12 specimens tested in the NIST laboratory are plotted (open diamond symbols) along with the E-glass data discussed above. When the break locations were fitted to a uniform distribution, 58% of the 12 specimens exhibited correlation coefficients at saturation of 0.999 or greater. However, all of the probability plot correlation coefficients of the carbon fiber SFC specimens were greater than 0.993. To verify the consistency of these results, the fragment length data at saturation from three additional laboratories were transcribed to yield relative break locations. The transcribed data are shown in Figure 4 along with the correlation coefficients obtained from the NIST data. Analyses of these data indicate that 43% of the 42 specimens tested yield correlations greater than 0.999, with all data exhibiting correlations greater than 0.991. It appears that the extensive debonding observed in the carbon fiber SFC specimens causes the fit of the fiber break locations to the uniform distribution to be very slightly reduced in these specimens. However, greater than 0.99x goodness-of-fit of these data to a uniform distribution suggests that the expected distribution of the ordered fragment lengths at saturation should conform to (1).

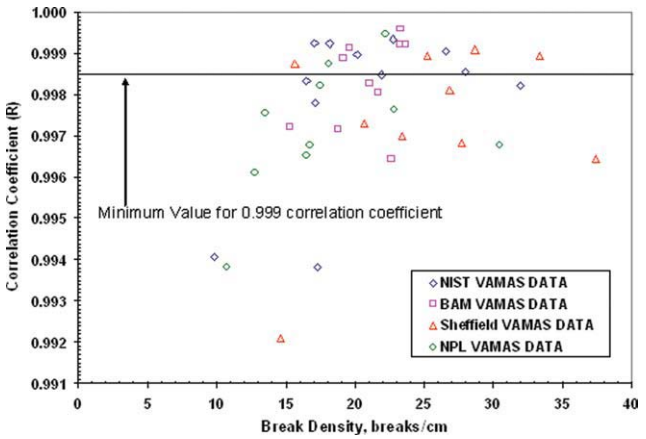

Figure 4 Correlation coefficients for fit of fiber break locations at saturation to the uniform distribution. All samples are AS-4 carbon fiber SFCs in DGEBA/*m*-PDA tested by VAMAS testing protocol for 2nd Round Robin Testing for the SFFT.[15] [Color figure can be viewed in the online issue, which is available at www.interscience.wiley.com.]

The effect of fiber–fiber interactions on fiber break spacings

To test the effect of fiber–fiber interactions on the sequential fragmentation process, combinatorial microcomposites were analyzed.[21] These specimens are composed of a 2D 6-fiber array sandwiched between two single fibers, with all the fibers being E-glass sized with aminopropyl trimethoxysilane (APTMS). Consistent with published data,[10] the separation distance between the array and the single fibers is greater than 300 μm, to minimize interaction between the 2D array and the single fibers, whose nominal diameter is 15 μm, whereas the interfiber spacing in the array is 21 μm. Unlike the unsized fibers, the APTMS sized fibers formed matrix cracks in the DGEBA/*m*-PDA matrix that led to premature failure of the combinatorial specimen through the interacting fiber breaks formed in the array.[22] To eliminate matrix crack formation in the combinatorial specimens, 20% of the molar amount of DGEBA was replaced with the same molar amount of diglycidyl ether of butanediol (DGEBD).

Consistent with the SFC test results, the distribution of fiber break locations in the multifiber array were also found to be uniformly distributed with goodness-of-fit correlation coefficients greater than 0.999 (Fig. 5). The fiber breaks in the two embedded single fibers, which were also uniformly distributed with correlation coefficients greater than 0.999, exhibited a higher number of breaks than the cluster fibers. These results are consistent with Li et al.[10] results from 2D Nicalon multifiber arrays and indicate that the expected outcome from the sequential fragmentation of interacting fibers is also uniform break locations, whose ordered fragment lengths according to statistical spacing theory should conform to (1). Furthermore, initial analyses of the break evolution process suggest that the onset of uniform break locations occurs at a lower break density than during the sequential fragmentation of single fibers. A detailed study of the fiber break evolution process in these multifiber arrays will be discussed in a future report to clarify the potential impact of this last observation.

The distribution of fragment lengths and SFC Weibull parameters

In the theories of Curtin[6] and Hui et al.,[7] Weibull parameters were extracted from the SFFT data. Researchers[23] have suggested that the validity of these parameters can be checked by fitting the cumulative distribution of the ordered fragment lengths at saturation, however, in practice, only fair agreement between predicted and measured results have been obtained. All the results of this article indicate from spacing theory[3,4] that the cumulative distribution of the ordered fragment lengths should conform to the distribution function given in (1). This suggests that the goodness-of-fit of the Weibull and lognormal distribution functions that have been used to fit the ordered fragment lengths at saturation are the result solely of the flexibility of the models used with no fundamental basis in physics or statistics. As a preliminary check of this conclusion, pooled data from the four E-glass DGEBA/*m*-PDA specimens tested by the slow test protocol[18] were fit using the continuous beta, lognormal, and three-parameter Weibull distribution functions (Fig. 6). The results indicate that the fits are comparable, with the three-parameter Weibull and lognormal functions giving slightly higher correlations than the continuous beta function. The two-parameter Weibull function, which is used to extract the Weibull parameters, was not flexible enough to provide a good fit of the data.

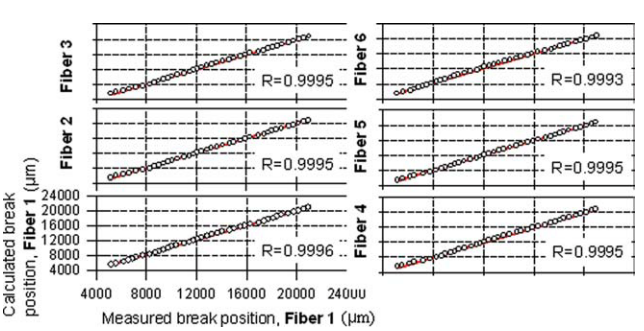

Figure 5 Uniform probability plots of cluster fiber breaks. The solid line represents the empirical fits. [Color figure can be viewed in the online issue, which is available at www.interscience.wiley.com.]

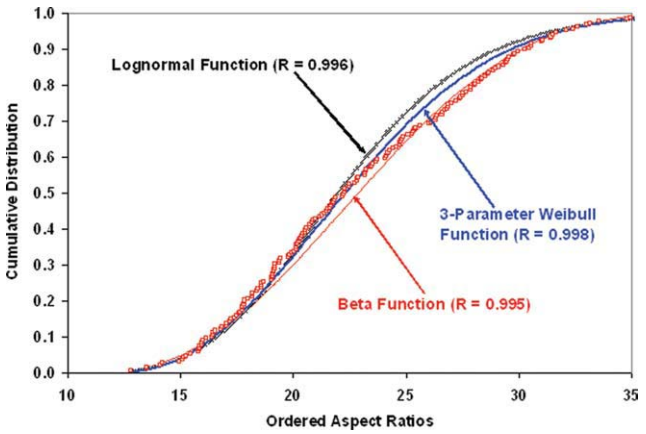

Figure 6 Fit of normalized ordered fragment lengths at saturation from specimens tested by the slow test protocol using the Beta, three-Parameter Weibull, and Lognormal functions. [Color figure can be viewed in the online issue, which is available at www.interscience.wiley.com.]

CONCLUSIONS

The experimental results discussed in this report strongly indicate that the expected outcome from the EFFT methodologies are fiber breaks whose locations conform to a uniform distribution. This outcome is found to be independent of adhesion strength, matrix type, fiber type, and fiber–fiber interactions. Uniform break locations from the sequential fracture of E-glass SFCs were found to exhibit goodness-of-fit correlations > 0.999, whereas those from carbon fiber SFCs display correlations >0.99. According to the theory of uniform spacings, the cumulative distribution of the ordered spacings (i.e., fragment lengths) from the uniform break locations conforms to a restricted discrete beta-like function whose exact form was derived by Whitworth.[3,4] Fits of this type of data by Weibull or lognormal distributions do not validate those models but rather reflect the flexibility of those functional forms. As a preliminary check of the Whitworth derivation, pooled data from four samples tested by the same protocol were fit by a continuous beta, three-parameter Weibull and lognormal distribution functions. Although all functions provided comparable fits of the data, the two-parameter Weibull function, which is used to extract Weibull parameters from the SFFT methodology, did not yield an acceptable fit.

Furthermore, the Kim et al.[2] results showing that the "exact" theories put forth by Curtin[6] and Hui et al.[7] do not accurately predict the fiber break density upto saturation are verified in this report. It is shown experimentally that the fragment lengths surviving to saturation decrease in size as saturation is approached rather than increase in size as predicted by the theories. Both theories assume that the matrix is elastic perfectly plastic (EPP assumption). Future work will focus on understanding this discrepancy by investigating the effect of nonlinear viscoelastic behavior of the polymer matrix using models such as those developed by Thuruthimattam et al.[24]

The authors like to thank Professor Andrew Rukhin, University of Maryland Baltimore County/National Institute of Standards and Technology (UMBC/NIST) for his many helpful comments during the preparation of this manuscript.

References

1. Wagner, H. D.; Steenbakkers, L. W. J Mater Sci 1989, 24, 3956.
2. Kim, J. H.; Leigh, S. D.; Holmes, G. Compos Sci Technol, submitted.
3. Pyke, R. J R Stat Soc B 1965, 27, 395.
4. Read, C. B. In Encyclopedia of Statistical Sciences; Kotz, S., Johnson, N. L., Eds.; Wiley: New York, 1988; Vol.8, p 566.
5. Gulino, R.; Phoenix, S. L. J Mater Sci 1991, 26, 3107.
6. Curtin, W. A. J Mater Sci 1991, 26, 5239.
7. Hui, C. Y.; Phoenix, S. L.; Ibnabdeljalil, M.; Smith, R. L. J Mech Phys Solids 1995, 43, 1551.
8. Bascom, W. D.; Jensen, R. M. J Adhes 1986, 19, 219.
9. Holmes, G. A.; Peterson, R. C.; Hunston, D. L.; McDonough, W. G.; Schutte, C. L. In Time Dependent and Nonlinear Effects in Polymers and Composites; Schapery, R. A., Ed.; American Society for Testing and Materials: West Conshohocken, Pennsylvania, 2000; pp 98–117.
10. Li, Z. F.; Grubb, D. T.; Phoenix, S. L. Compos Sci Technol 1995, 54, 251.
11. Kim, J.-H.; Holmes, G. A. In Proceedings 27th Annual Meeting of the Adhesion Society, Inc.; Chaudhury, M. K., Anderson, G. L., Eds.; The Adhesion Society: Blackburg, Virginia, 2004; p 525.
12. Cox, H. L. Br J Appl Phys 1952, 3, 72.
13. Rosen, W. B. In Fiber Composite Materials; American Society of Metals, Ed.; American Society of Metals: Metals Park, OH, 1965; Chapter 3, p 37.
14. Rosen, W. B.; Dow, N. F.; Hashin, Z. Mechanical Properties of Fibrous Composites, NASA CR-31; General Electric Company: Philadelphia, PA, 1964.
15. Rich, M. J.; Drzal, L. T.; Hunston, D. L.; Holmes, G.; McDonough, W. G. In Proceedings of the American Society for Composites; Sun, C. T., Kim, H., Eds.; CRC Press LLC: Boca Raton, FL, 2002; p 158.
16. Holmes, G. A.; Peterson, R. C.; Hunston, D. L.; McDonough, W. G. Polym Compos 2007, 28, 561.
17. Holmes, G. A.; Feresenbet, E.; Raghavan, D. In Proceedings of the 24th Annual Meeting of the Adhesion Society; Emerson, J. A., Ed.; The Adhesion Society: Blacksburg, VA 24061-0201, 2001; p 62.
18. Holmes, G. A.; Peterson, R. C.; Hunston, D. L.; McDonough, W. G. Polym Compos 2000, 21, 450.
19. Holmes, G. A.; Feresenbet, E.; Raghavan, D. Compos Interfac 2003, 10, 515.
20. McDonough, W. G.; Holmes, G. A.; Peterson, R. C. In Proceedings of the 13th Technical Conference on Composite Materials; American Society for Composites: Baltimore, 1998; p 1688.
21. Kim, J.-H.; Hettenhouser, J. W.; Moon, C. K.; Holmes, G. A. Compos Sci Technol, submitted.
22. Holmes, G. A.; McDonough, W. G. In Proceedings of the 47th International SAMPE Symposium and Exhibition; Rasmussen, B. M., Pilato, L. A., Kliger, H. S., Eds.; Society for the Advancement of Material and Process Engineers (SAMPE): Covina, CA, 2002; p 1690.
23. Zhao, F. M.; Takeda, N. Compos Part A Appl Sci Manuf 2000, 31, 1215.
24. Thuruthimattam, B. J.; Waas, A. M.; Wineman, A. S. Int J Non Lin Mech 2001, 36, 69.